Novel approaches in 3D live cell microscopy

V. Richter, M. Rank, A. Heinrich, H. Schneckenburger

Abstract. **Microscopy methods for 3D live cell imaging, including various techniques, challenges and restrictions, are described. Novel devices for application of these methods in combination with 3D printed optics are presented and discussed.**

Keywords: 3D microscopy, fluorescence, light sheet, 3D printed optics.

1. Introduction

For experimental and pre-clinical life cell studies two-dimensional (2D) cell cultures are traditionally used, as they are easy to establish, but frequently provide results of limited significance, since cells are lacking a physiological microenvironment. In contrast, three-dimensional (3D) cell cultures, e.g. multicellular tumour spheroids, maintain tissue-like properties and, therefore, provide a more realistic background for experimental studies, e.g. tissue diagnostics or screening of pharmaceutical agents [1, 2]. 3D cultivation techniques commonly prevent cell attachment to surfaces, using e.g. hanging drop methods or specific coatings of these surfaces. 3D spheroids can be grown from various kinds of cells, e.g. cells from kidney, breast, liver and other organs (for a review see e.g. [3, 4]). Although 3D systems often lack a vasculature, which might support tissues with oxygen and nutrients, fully vascularised organoids [5] have been reported in recent studies. In the present paper, experiments with 3D spheroids of Chinese Hamster Ovary cells expressing a membrane associated green fluorescent protein (CHO-pAcGFP1-Mem) are reported.

Main problems of imaging 3D specimens are that the sample thickness commonly exceeds the depth of focus of a conventional microscope, and that light scattering affects the image quality. Therefore, methods based on optical sectioning, e.g. confocal laser scanning microscopy (CLSM) [6, 7], structured illumination microscopy [8], or light sheet fluorescence microscopy (LSFM) [9, 10] are applied preferentially. Here, images are recorded plane by plane, and resulting 3D plots are calculated offline. A challenge is location of 3D sam-
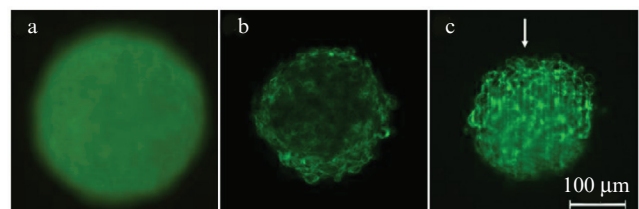
ples in a microscope using e.g. specific cuvettes [11] or micro-wells on chamber slides (https://ibidi.com). This paper describes the possibility of fabricating micro-wells on microscope object slides or coverslips by additive manufacturing and of using these 3D printed optics for location and imaging of 3D tumour spheroids.

2. Microscopy techniques

2.1. Methods

Often the diameter of 3D specimens (typically no less than 100 nm) exceeds considerably the depth of focus of a conventional microscope. Therefore, a conventional wide-field image is composed by an image from the focal plane and numerous out-of-focus images, so that the resulting image is rather blurred, as demonstrated in Fig. 1a. To increase image quality, methods of optical sectioning are used either in a wide-field or in a scanning mode. In confocal laser scanning microscopy (CLSM), a laser beam scans the sample point by point, thus creating a two-dimensional image within typically a few seconds. A spatial pinhole in a conjugate image plane blocks out-of-focus light and permits a sectional image with high contrast, as depicted in Fig. 1b. Information (e.g. fluorescence) from individual planes is then used for 3D image reconstruction by appropriate software. However, the whole procedure needs comparatively long scanning times and high light exposure, which may damage living specimens.

Alternative imaging techniques are based on wide-field microscopy. Optical sectioning structured illumination microscopy (OS-SIM) [8] is an appropriate technique to sepa-

V. Richter, H. Schneckenburger Institute of Applied Research Aalen University, 73430 Aalen, Germany;
e-mail: herbert.schneckenburger@hs-aalen.de;
M. Rank, A. Heinrich Center for Optical Technologies (ZOT), Aalen University, 73430 Aalen, Germany

Figure 1. (Colour online) Spheroids of CHO-pAcGFP1-Mem cells recorded by (a) conventional fluorescence microscopy, (b) confocal laser scanning microscopy and (c) light sheet fluorescence microscopy. Single planes are selected in (b) and (c) at a depth of 60 μm; the arrow indicates direction of light incidence (excitation wavelength: 488 nm; fluorescence detected at $\lambda \geqslant 505$ nm). Reproduced from [12] with modifications.

rate in-focus information from signals generated in out-of-focus planes. To achieve this, an optical grid is imaged in the plane of the sample in three phase positions: $\Phi_1 = 0$, $\Phi_2 = 2\pi/3$ and $\Phi_3 = 4\pi/3$ resulting in the intensities I_1, I_2 and I_3. An algorithm $I = [(I_1 - I_2)^2 + (I_1 - I_3)^2 + (I_2 - I_3)^2]^{1/2}$ permits calculating an image from the focal plane, while out-of-focus images add up to zero, as visualised elsewhere [12]. Upon variation of the sample's vertical position, several focal planes can thus be measured, and a 3D image may be calculated. Total acquisition time and light exposure is similar to CLSM, and again the risk of damaging living specimens is rather high. This problem may be overcome by light sheet fluorescence microscopy (LSFM). Here, the sample is illuminated from the side (at 90° with respect to the microscope axis) by either a cylindrical lens or scanning of a laser beam. For 3D imaging, the light sheet and the microscope objective lens used for detection are shifted simultaneously in axial direction, so that the illuminated part of the sample is always in the focus of the objective lens (Fig. 1c). Thus, z-stacks can be recorded with low fluorescent background prior to calculation of a 3D image. The main advantage of LSFM over OS-SIM is that only those planes are illuminated, which are recorded simultaneously, so that light exposure is considerably lower. Commercial light-sheet microscopes (e.g. Carl Zeiss, Olympus, Nikon), as well as open-source solutions or add-ons for existing microscopes are presently available [13, 14]. Light sheet fluorescence microscopy was recently combined with further innovative techniques, e.g. spectral imaging or fluorescence lifetime imaging (FLIM) using time-correlated single photon counting (TCSPC) [15] as well as fast camera technologies in the time [16] or frequency domains [17].

2.2. Challenges and restrictions

A major problem in imaging of 3D cell cultures is light scattering, which reduces the quality of images due to light attenuation, blurring and a loss of contrast. Obviously, these problems are more severe for three-dimensional samples than for two-dimensional ones, since scattering does not only occur in a certain plane of detection, but also creates background signals from the whole illuminated specimen. Methods of optical sectioning (see above) reduce the influence of scattering, as also documented by Fig. 1. However, CLSM generally reduces the fluorescence intensity in deeper layers of the specimen, and LSFM shows an increasing effect of scattering in the direction of beam propagation. Also some stripes in the direction of light incidence appear to be unavoidable in this case (Fig. 1c). Further reduction of light scattering can be achieved by using higher wavelengths of illumination with a lower scattering coefficient (e.g. in multiphoton microscopy [18, 19]) or by matching the refractive indices of sample and surrounding medium. These 'clearing techniques' are used increasingly for deep view imaging of skin, brain and other organs and can also be applied to 3D spheroids [20], but generally are not compatible with live cell imaging.

All sectioning methods require multiple light exposures, but only for LSFM each image results from only one illuminated plane, whereas for all other wide-field and laser scanning techniques, the whole specimen has to be illuminated for detection of each sectional image. This implies that light exposure for obtaining a 3D image is summing up and often exceeds the limit of non-phototoxic light doses. Tolerable light doses were determined in a previous paper [21] and ranged between 25 J cm^{-2} (375 nm) and 200 J cm^{-2} (633 nm) for cultures of native cells, corresponding to 4 min up to about 30 min of solar irradiance (around 100 mW cm^{-2}). If cells were stained with a fluorescent dye or transfected with a fluorescent protein, typical non-phototoxic light doses were only around 10 J cm^{-2}, corresponding to 100 s of solar irradiance. While only about 20 layers of a 3D cell spheroid can thus be irradiated by CLSM, a large number of layers can be illuminated about 100 times each by LSFM. This favours light sheet microscopy for long-term observation. However, light sheet microscopy requires illumination of the samples from the side and, therefore, needs specific sample holders. While micro-cuvettes or commercial multi-well chamber slides (see above) appear to be appropriate devices, routine applications require more flexible, cheaper and disposable components. Therefore, we are presently testing whether 3D printed micro-optics might fulfil these requirements. First papers concerning the use of 3D printed optics for light sheet microscopy in connection with hydrogels were previously reported [22, 23]; however, it was our aim to apply a more general concept, which might be appropriate for any kind of 3D cell or tissue samples.

3. D Printed Optics

3.1. Methods

The main requirements for 3D printed sample holders are as follows:
– use of standard printing procedures for micro-chambers on a microscope object slide or coverslip;
– small inner volume with perpendicular walls; and
– high transparency and low scattering of the printed material.

In particular, the small inner volume is necessary for precise localisation of the sample and for saving (expensive) culture media or reagents, while the perpendicular and transparent chamber walls are needed for a high quality of the light sheet. In the present case, a standard projection micro-stereolithography (PµSL) system (Autodesk Ember) was used to print squares of 2×2 mm inner surface, 0.1 mm height and a wall thickness of 0.5 mm, as depicted in Fig. 2. UV sensitive resin was cured locally layer by layer, defined by a digital micro-mirror device (dmd) mask. The layered process requires for the walls of the cell compartment to be multiples pixel wide. Both the wall width and the layers cause scattering, which affect the microscopy measurements. Therefore, a modified printing system was set up, which enables much thinner walls for better clarity. The custom 3D printer uses the dmd unit from the PµSL-system to cure the mask in a droplet of resin between two substrates in one layer. As the UV light penetrates the resin through one substrate, it sticks to it, while with the appropriate settings (irradiance and duration of exposure) the other substrate can be removed afterwards to wash off any uncured resin. While Fig. 2a shows the principal use for light sheet as well as for conventional microscopy, Fig. 2b shows 3D printed micro-chambers from the custom setup on a microscope object slide. Single micro-wells or micro-chambers arranged in series can be used; the only prerequisite is that they should be accessible by a light sheet produced by either a cylindrical lens or a focused scanning laser beam.
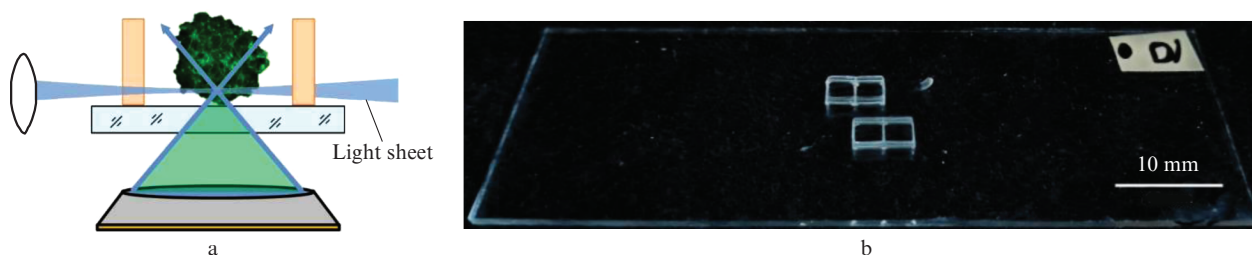
Figure 2. (Colour online) (a) Scheme of a 3D printed sample holder (micro-chamber) for light sheet and conventional microscopy of a cell spheroid; (b) layout of 3D printed micro-chambers on a microscope object slide.

3.2. Applications

Using the 3D printed micro-chambers we performed test experiments with a light sheet module adapted to an inverted fluorescence microscope (Axiovert 200M, Carl Zeiss Jena, Germany) and a photonic crystal fibre laser (NKT Photonics SuperK EXTREME with SuperK VARIA tunable single line filter,) operated at (470 ± 20) nm and emitting unpolarised light, as described in detail elsewhere [13]. For testing the quality of the light sheet we rotated the focusing cylindrical lens by 90°, so that the light sheet was oriented vertically. The micro-well was filled with a fluorescent solution (rhodamine 6G, 2.5 µM), so that by simultaneous fluorescence and transmission microscopy we could visualise the beam waist, as demonstrated in Fig. 3. At a distance of -100 µm to $+100$ µm from the focus of the laser beam this waist did not exceed 10 µm as reported recently for micro-capillaries [13]. However, in contrast to the capillaries the beam depicted in Fig. 3 showed some singularities (luminescent spots) due to scattering at the chamber wall as well as at some impurities on its bottom, which can also be seen in Fig. 3, and which result from the process of additive manufacturing.
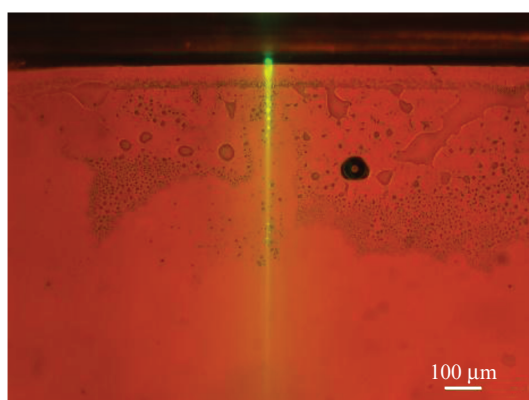
Figure 3. (Colour online) Light sheet in a 3D printed well containing a solution of rhodamine 6G (2.5 µM); transmission and fluorescence microscopy ($1010^{\times}/0.30$ objective lens, $\lambda_{ex} = 450-490$ nm, $\lambda_{em} \geqslant 515$ nm). On top of the well, part of the chamber wall is depicted.

When the light sheet was rotated back to a horizontal position, the laser beam did no longer hit the bottom of the micro-well, and illumination was more homogeneous. LSFM was then applied to spheroids of CHO-pAcGFP1-Mem cells in vertical steps of 10 µm, as depicted in Fig. 4. This Figure shows various cell layers with membrane associated green fluorescence at different distances from the bottom of the well including some shadow in the central part of the spheroid due to attenuation of incident and fluorescence light. The quality of the individual images as well as their 3D projection (Fig. 4) is similar to that in micro-cuvettes [13]. Recording time for each layer was 1 s, and total light exposure was far below a critical level of phototoxicity of 10 J cm^{-2} [21].

4. Discussion and perspectives

3D printed wells on microscope object slides, as reported in this paper, are an attractive alternative to micro-capillaries or customary chamber-slides for localisation of cell spheroids under physiological conditions. In particular, for light sheet microscopy they offer numerous advantages, but they appear also appropriate for conventional transmission or fluorescence microscopy. When high aperture objective lenses are used, the microscope object slide has to be replaced by a thinner plate, e.g. coverslip, and then mechanical stability is an important issue. Furthermore, with increasing magnification purity and homogeneity of the bottom of the micro-wells plays an important role.

3D printed micro-wells can also be used for super-resolution microscopy with a resolution below the Abbe or the Rayleigh criterion. Meanwhile, stimulated emission depletion (STED) microscopy [24] and single molecule localisation microscopy (SMLM) [25, 26] are well established methods, but most commonly limited to sample surfaces. Super-resolution structured illumination microscopy (SR-SIM) with 2 or 3 interfering laser beams has the potential for application to 3D cell cultures. However, due to light scattering the contrast of the interference pattern is generally lost at depths above about 20 µm (as also confirmed by own experiments [27]), so that the method is again restricted to cell layers close to the sample surface. A higher penetration depth up to about 100 nm has been reported for lattice light sheet microscopy [28], and its use in combination with 3D printed optics would appear promising. A good compromise would be the application of enhanced methods of CLSM, with a pinhole being replaced by a larger number of detector devices (Airy Scan Microscopy or Image Scan Microscopy). Here, deep view imaging would appear possible at a resolution of 100–200 nm, and application of 3D printed optics to cell spheroids or small biopsies is quite promising.
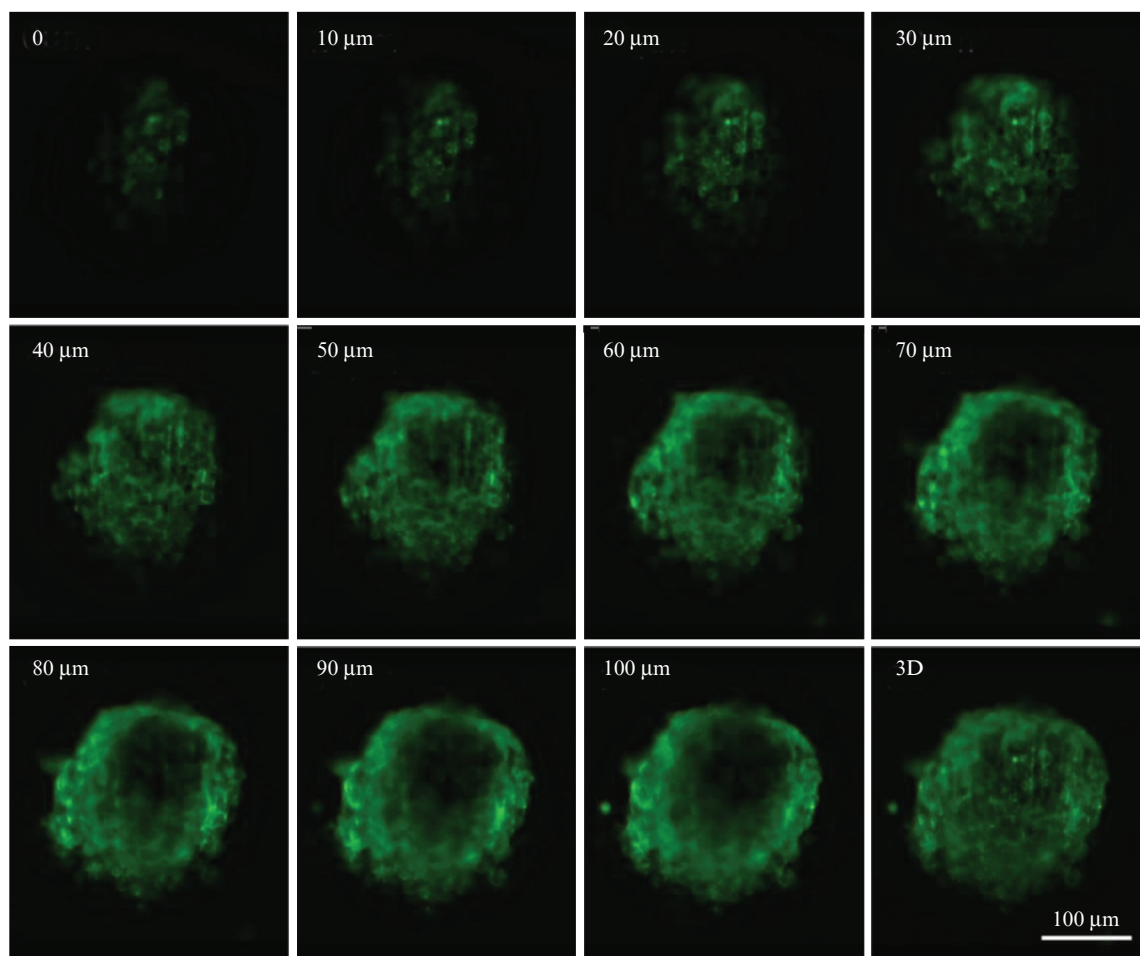
Figure 4. (Colour online) Light sheet microscopy of a CHOpAcGFP1-Mem cell spheroid in a 3D printed well at distances between 0 and 100 μm (increments of 10 μm) from the bottom of the well including 3D reconstruction; well dimensions: $1.5 \times 1.5 \times 1$ mm; wall thickness: 1 mm; $10^\times/0.3$ objective lens; $\lambda_{ex} = 450 - 490$ nm, $\lambda_{em} \geqslant 515$ nm.

References

1. Kunz-Schughart L.A., Freyer J.P., Hofstaedter F., Ebner R. *J. Biomol. Screening*, **9**, 273 (2004); https://doi.org/10.1177/1087057104265040.

2. Wittig R., Richter V., Wittig-Blaich S., Weber P., Strauss W.S.L., Bruns T., Dick T.-P., Schneckenburger H. *J. Biomol. Screening*, **18**, 736 (2013); https://doi.org/10.1177/1087057113480525.

3. Van Ineveld R.L., Ariese H.C.R., Wehrens E.J., Dekkers J.F., Rios A.C. *J. Vis. Exp.*, **5** (160), e60709 (2020); https://doi.org/10.3791/60709.

4. Torres S., Abdullah Z., Brol M.J., Hellerbrand C., Fernandez M., Fiorotto R., Klein S., Königshofer P., Liedtke C., Lotersztajn S., Nevzorova Y.A., Schierwagen R., Reiberger T., Uschner F.E., Tacke F., Weiskirchen R., Trebicka J. *Int. J. Mol. Sci.*, **21** (6), 2027 (2020); https://doi.org/10.3390/ijms21062027.

5. Mansour A.A., Gonçalves J.T., Bloyd C.W., Li H., Fernandes S., Quang D., Johnston S., Parylak S.L., Jin X., Gage F.H. *Nat. Biotechnol.*, **36**, 432 (2018); https://doi.org/10.1038/nbt.4127.

6. Pawley J. *Handbook of Biological Confocal Microscopy* (Boston, MA, USA: Springer, 1990); https://doi.org/10.1007/978-0-387-45524-2.

7. Webb R.H. *Rep. Prog. Phys.*, **59**, 427 (1996); https://doi.org/10.1088/ 0034-4885/59/3/003.

8. Neil M.A., Juskaitis R., Wilson T. *Opt. Lett.*, **22** (24), 1905 (1997); https://doi.org/10.1364/OL.22.001905.

9. Pampaloni F., Chang B.-J., Stelzer E.H.K. *Cell Tissue Res.*, **362** (1), 265 (2015); https://doi.org/10.1007/s00441-015-2144-5.

10. Santi P.A. *J. Histochem. Cytochem.*, **59** (2), 129 (2011); https://doi.org/ 10.1369/0022155410394857.

11. Bruns T., Schickinger S., Schneckenburger H. *J. Vis. Exp.*, **90**, e51993 (2014); https://doi.org/10.3791/51993.

12. Schneckenburger H., Richter V. *Photonics*, **8**, 275 (2021); https://doi.org/10.3390/photonics8070275.

13. Bruns T., Bauer M., Bruns S., Meyer H., Kubin D., Schneckenburger H. *J. Microsc.*, **264** (3), 261 (2016); https://doi.org/10.1111/jmi.12439.

14. Greger K., Swoger J., Stelzer E.H.K. *Rev. Sci. Instrum.*, **78**, 023705 (2007); https://doi.org/10.1063/1.2428277.

15. Hirvonen L.M., Nedbal J., Almutairi N., Phillips T.A., Becker W., Conneely T., Milnes J., Cox S., Stürzenbaum S., Suhling K. *J. Biophotonics*, **13** (2), e201960099 (2020). DOI: 10.1002/jbio.201960099.

16. Weber P., Schickinger S., Wagner M., Angres B., Bruns T., Schneckenburger H. *Int. J. Mol. Sci.*, **16** (3), 5375 (2015). DOI: 10.3390/ijms16035375.

17. Mitchell C.A., Poland S.P., Seyforth J., Nedbal J., Gelot T., Huq T., Holst G., Knight R.D., Ameer-Beg S.M. *Opt. Lett.*, **42** (7), 1269 (2017). DOI: 10.1364/OL.42.001269.

18. König K. *J. Microsc.*, **200** (Pt 2), 83 (2000); https://doi.org/10.1046/j.1365-2818.2000.00738.x.

19. Miller D.R., Jarrett J.W., Hassan A.M., Dunn A.K. *Curr. Opin. Biomed. Eng.*, **4**, 32 (2017); https://doi.org/10.1016/j.cobme.2017.09.004.

20. Costa E.C., Silva D.N., Moreira A.F., Correia I. *Biotechnol. Bioeng.*, **116** (19), 2742 (2019); https://doi.org/10.1002/bit.27105.

21. Schneckenburger H., Weber P., Wagner M., Schickinger S., Richter V., Bruns T., Strauss W.S.L., Wittig R. *J. Microsc.*, **245**, 311 (2012); https://doi.org/10.1111/j.1365-2818.2011.03576.x.
22. Desmaison A., Lorenzo C., Rouquette J., Ducommun B., Lobjois V. *J. Microsc.*, **251** (2), 128 (2013). DOI: 10.1111/jmi.12051.
23. Jeandupeux E., Lobjois V., Ducommun B. *Biochem. Biophys. Res. Commun.*, **463** (4), 1141 (2015). DOI: 10.1016/j.bbrc.2015.06.072.
24. Wildanger D., Medda R., Kastrup L., Hell S.W. *J. Microsc.*, **236** (1), 35 (2009). DOI: 10.1111/j.1365-2818.2009.03188.x.
25. Betzig E., Patterson G.H., Sougrat R., Lindwasser O.W., Olenych S., Bonifacino J.S., Davidson M.W., Lippincott-Schwartz J., Hess H.F. *Science*, **313** (5793), 1642 (2006). DOI: 10.1126/science.1127344.
26. Rust M.J., Bates M., Zhuang X. *Nat. Methods*, **3** (10), 793 (2006). DOI: 10.1038/nmeth929.
27. Schneckenburger H., Richter V., Gelleri M., Ritz S., Vaz Pandolfo R., Schock F., von Hase J., Birk U., Cremer C., *Quantum Electron.*, **50** (1), 2 (2020) [*Kvantovaya Elektron.*, **50** (1), 2 (2020)].
28. Chen B.C. et al. *Science*, **346** (6208), 1257998 (2014). DOI: 10.1126/science.1257998.